PAPER

Check for updates

Electrochemical interface based on polydopamine and gold nanoparticles/reduced graphene oxide for impedimetric detection of lung cancer cells†

Nguyen Dieu Linh, [ID] [a] Nguyen Thi Trang Huyen,[a] Nguyen Hai Dang,[a] Benoit Piro[b] and Vu Thi Thu [ID] *[a]

The use of non-invasive approaches for monitoring therapy processes in cancer patients at late stages is truly needed. In this work, we aim to develop an electrochemical interface based on polydopamine combined with gold nanoparticles and reduced graphene oxide for impedimetric detection of lung cancer cells. Gold nanoparticles (around 75 nm) were dispersed onto reduced graphene oxide material pre-electrodeposited onto disposable fluorine doped tin oxide electrodes. The coordination between gold and carbonaceous material has somehow improved the mechanical stability of this electrochemical interface. Polydopamine was later introduced onto modified electrodes *via* self-polymerization of dopamine in an alkaline solution. The result has demonstrated the good adhesion and biocompatibility of polydopamine towards A-549 lung cancer cells. The presence of the two conductive materials (gold nanoparticles and reduced graphene oxide) has led to a six-times decrease in charge transfer resistance of polydopamine film. Finally, the as-prepared electrochemical interface was employed for impedimetric detection of A-549 cells. The detection limit was estimated to be only 2 cells per mL. These findings have proved the possibilities to use advanced electrochemical interfaces for point-of-care applications.

Introduction

Circulating tumor cells (CTCs) that detach from the tumor lesion and then travel in the blood stream during tumor metastasis are an important biomarker for monitoring cancer stages and validating cancer treatment processes.[1] Commonly used methods for detecting CTCs mainly include immuno-magnetic beads[2] and microfluidic technologies.[3] For instance, the Cell Search system, the only FDA-approved product for CTC detection, is based on the enrichment of cells overexpressing epithelial cell adhesion molecule (EpCAM) on magnetic beads pre-modified with antibodies. These methods share some main drawbacks such as high-cost instrumentation, extensive protocols, long analysis time, and expensive reagents. Several sensing systems were also employed for rapid detection of CTCs such as field effect transistors,[4,5] chemiluminescence,[6,7] photo-electrochemistry,[8] fluorescence,[9] Raman,[10] surface plasmon resonance,[11] immucytochemical staining.[12] Among them, electrochemical sensors are becoming more prominent in CTC

detection not only for their rapidity, simplicity, portability and high sensitivity but also their ability to be adapted to electronic devices.[13]

To date, most of the electrochemical platforms reported for cytosensing purposes have been based on immunosensors or aptasensors. In 2021, He Su *et al.* demonstrated a three-dimensional graphene/ZnO macroporous structure modified with anti-EpCAM for detection of breast cancer cell MCF-7.[14] An electrochemical cytosensor based on gold nanoparticles and carbon nanosphere has been reported for voltammetric detection of lung cancer cell A-549.[15] A sandwich-type electrochemical immunosensor in which the capture antibody was immobilized on gold nanoparticles/acetylene black film whereas the signal antibody was decorated with Pt@Ag nanoflowers was developed by Sitian Tang *et al.* to detect MCF-7 in 2018.[16] The electrochemical signal resulting from H_2O_2 reduction can be amplified with the aid of Pt@Ag nanostructure due to its intrinsic horseradish peroxidase activity and then recorded using differential pulse voltammetry technique (DPV). Electrochemical immunosensor in sandwich-format was also adapted to detect other antigens over-expressed in patients with cancer such as human epidermal growth factor receptor 2 (breast cancer),[17] squamous cell carcinoma antigen (skin cancer),[18] alpha-fetoprotein (hepatocellular carcinoma),[19] or even the whole cell.[20] Although these immunoassays exhibit high sensitivity and good specificity, they are quite time-consuming, require expensive reagents and strict storage

[a]University of Science and Technology of Hanoi (USTH), Vietnam Academy of Science and Technology (VAST), 18 Hoang Quoc Viet, Cau Giay, Hanoi, Vietnam. E-mail: thuvu.edu86@gmail.com; vu-thi.thu@usth.edu.vn

[b]Université Paris Cité, ITODYS, CNRS, UMR 7086, 15 Rue J.-A. de Baïf, Paris, F-75013 France

† Electronic supplementary information (ESI) available. See DOI: https://doi.org/10.1039/d3ra00793f

conditions for antibodies. The use of aptamers, artificial oligonucleotides selected by systematic evolution of ligands by exponential enrichment (SELEX), might help to overcome these issues. Mahdi Sadeghi[21] has shown an electrochemical aptasensor based on graphene sheets decorated with Rhodium nanoparticles to detect HER2-ECD (oncomarker for breast cancer). The selected anti-HER2 aptamer strand made up 54 oligonucleotide bases was fixed on the electrode surface, ready to recognize HER2-ECD oncomarker *via* G-quadruplex formation between them. Xiaoyan Zhou *et al.* has even utilized AS1411 aptamer (a nucleolin-targeting aptamer) as probe antibodies to detect HeLa cell in sandwich-format immunoassay.[22] Still, it is needed to undergo a time-consuming procedure to select as well as synthesize suitable aptamers.

Recently, electrochemical cytosensors which do not use either antibodies or aptamers, but directly detect the targeted cells in a label-free manner are highly desirable. In 2021, a biodetection system for A-549 lung cancer cells using biomimetic polydopamine (PDA) was proposed by Bolat *et al.*[23] It was reported that PDA modified electrode is a good platform for rapid and label-free detection of A-549 cells in the concentration range from 10^2 to 10^5 cells per mL with a low detection limit of 25 cells per mL. Despite of the good adhesive property,[24] the low conductivity and slow electron transfer at PDA layer might still somehow affect to the recorded signals. Thus, some more conductive nanostructures with good biocompatibility such as gold nanoparticles and carbonaceous materials[25,26] should be employed. In this work, we aim to develop an impedimetric cytosensor based on polydopamine in combination with gold nanoparticles (AuNPs) and reduced graphene oxide (rGO). An electrochemical platform based on electrochemically reduced graphene oxide and electro-deposited gold nanoparticle were first prepared to ensure good electron transfer rate at electrode surface. Herein, the presence of carbonaceous matrix (rGO) might help to prevent aggregation, thus providing more homogenously distributed AuNPs. The use of gold particles is probably beneficial to improve electron transfer rate at electrode surface. Polydopamine (PDA) was introduced onto AuNPs/ rGO hybrid film by self-polymerization of dopamine in alkaline conditions. As usual, this PDA coating probably enhanced the adhesion of cells onto electrode surface, thus improving sensing performances of the as-developed sensor. Electrochemical impedance spectroscopy (EIS), a versatile and non-destructive technique, will be further used to analyze CTCs in a label-free manner.

Experimental

Materials and apparatus

Dopamine hydrochloride (DA-HCl) (MW = 189.6), phosphate buffer saline (PBS) tablet, potassium hexacyanoferrate(III) ($K_3[Fe(CN)_6]$, MW = 329.2), potassium hexacyanoferrate(II) ($K_4[Fe(CN)_6] \cdot 3H_2O$, MW = 422.4), and gold(III) chloride trihydrate ($HAuCl_4 \cdot 3H_2O$, MW = 393.8), fluorine doped tin oxide coated glass electrode (FTO electrode) ($L \times W \times$ thickness = 100 mm × 100 mm × 2.3 mm, surface resistivity ∼7 Ω sq^{-1}) were purchased from Sigma-Aldrich. Cell culture plate

(96 wells, 07-6096) were purchased from Biologix and lung adenocarcinoma cell line (A-549) was purchased from (American Type Culture Collection (ATCC). Graphene oxide (GO) was prepared by our research group using Hummer's methods.

Preparation of PDA/AuNPs/rGO modified FTO electrode

Before being modified, FTO electrodes were cleaned carefully in Piranha solution ($H_2SO_4 : H_2O_2 = 3 : 1$). Then, all the FTO electrodes were cleaned thoroughly with distilled water several times to remove excess acid. After being dried, clean FTO electrodes were coated with a thin layer of transparent nail polish as a nonconductive layer, making the area of the FTO working surface become fixed (1 × 1 cm^2).

AuNPs/rGO hybrid film was prepared using electrochemical approach as described in our previous works.[27–29] Firstly, rGO was deposited by cyclic voltammetry (CV) from GO dispersion in aqueous condition. The reduction was performed in 1 mg mL^{-1} GO dispersion in PBS (pH 7.4) by scanning 20 cycles from −1.2 V to 0 V (*vs.* Ag/AgCl) at a scan rate of 50 mV s^{-1}. The rGO deposited FTO was then rinsed with double distilled water and let dry at room temperature. After that, 2 mM $HAuCl_4 \cdot 3H_2O$ in aqueous 0.25 M Na_2CO_3 solution was used to deposit AuNPs onto the rGO/FTO electrode surface in a potential range from −0.9 V to 0.2 V at a scan rate of 50 mV s^{-1}. Finally, the PDA adhesive layer was introduced by immersing AuNPs/rGO/FTO in tris solution (pH 8.5) containing dopamine hydrochloride (DA-HCl) (2 mg mL^{-1}) under a constant magnetic stirring for 60 minutes.

Morphology and structure studies

FE-SEM images (field emission scanning electron microscopy) were captured by using S-4800 system (Hitachi, Japan) operating at 5.0 kV accelerating voltage. Structural behaviours of the samples were examined using Fourier Transform Infrared spectrometer (Nicolet™ iS50, Thermo-Scientific) and Raman spectrometer (Lab-ram, Horiba, Japan, excitation laser 532 nm).

Electrochemical behaviors

All the electrochemical measurements were carried out with Autolab – PGSTAT302 potentiostat/galvanostat instrument controlled by NOVA software (Autolab, Switzerland) and a three-electrode system with an Ag/AgCl (3 M KCl) reference electrode, platinum wire counter electrode, and a FTO working electrode. Cyclic voltametric (CV) measurements were performed in a redox probe solution of 5 mM $Fe(CN)_6^{3-/4-}$ in phosphate buffer solution (PBS, pH 7.4) by scanning from −0.6 V to 0.9 V (*vs.* Ag/AgCl) at a scan rate of 100 mV s^{-1}. The electrochemical impedance spectroscopy (EIS) measurements were performed in the same redox probe solution with a frequency range from 0.01 Hz to 100 kHz at AC potential of 0.3 V with a sinusoidal amplitude of 10 mV. By using the electrochemical fitting program of Autolab – PGSTAT302 potentiostat, the elements of Randles circuit values were calculated.

Cell viability – MTT test

The viability of the cells on polydopamine film were tested using MTT assay at high cell concentration of 10^5 cells per mL. Firstly, polydopamine was introduced to several wells in 96-wells plate by self-polymerization of dopamine solution in alkaline condition. The wells modified with polydopamine film were all treated under UV light for 2 hours in order to avoid unwanted contaminants. Then, the treated wells were incubated with 200 µL A-549 cell suspension in PBS (pH 7.4) for 48 h at 37 °C. After that, they were rinsed with PBS (pH 7.4) and dried for 30 minutes in a 37 °C incubator. The presence of cells onto the as-prepared surfaces can be examined using a high-resolution microscope. Finally, 20 µL MTT solution was added to each well and incubated for 3 hours at 37 °C, the medium was aspirated, and then 200 µL of isopropyl alcohol (IPA) was added to each well to dissolve formazan crystals. The MTT assay result was obtained by using SpectraMax iD5.

Cell detection

After the adhesion of A-549 lung cancer cells with different concentrations (10^1 to 10^4 cells per mL) on PDA/AuNPs/rGO modified FTO electrodes, cell detection will be conducted using EIS technique. All the EIS measurements were conducted in 5 mM $Fe(CN)_6^{3-/4-}$ in PBS (pH 7.4) with a frequency range from 0.01 Hz to 100 kHz at AC potential of 0.3 V with a sinusoidal amplitude of 10 mV.

Results and discussions

Preparation of PDA/AuNPs/rGO/FTO

The aim of this work is to prepare a PDA/AuNPs/rGO hybrid film on FTO electrodes for further cytosensing applications towards lung cancer cells. The PDA layer is needed to ensure the adhesion of the cells on the electrode surfaces. The gold material is beneficial to improve the charge transfer whereas the rGO supporting layer might help to have a better dispersion of gold nanoparticles. Meanwhile, the AuNPs/rGO might also facilitate the immobilization of the cells and somehow enhance the mechanical stability of the film.

The formation of each material layer onto FTO electrode can be seen by naked eyes. While both rGO and PDA are in dark colour, AuNPs exhibits a common shiny pink colour (Fig. S1†). The color of the oxidizing dopamine solution also changed from light orange to dark brown (Fig. S2†). During the time of reaction, PDA was obtained in solution by oxidative self-polymerization of dopamine[30] in tris solution (pH 8.5) – an alkaline aqueous buffer solution, and at the same time, the electrodes were coated by PDA.

Cyclic voltammetry method was chosen to deposit rGO and AuNPs since we can easily observe the formation of these two materials onto the electrode surface *via* cyclic voltammograms. The GO with oxygenated moieties was irreversibly reduced to rGO at negative potentials[27,29] (data not shown here). Cyclic voltammograms recorded during the growth of AuNPs onto rGO modified electrode (Fig. 1) shows one peak related to bulk deposition (BD) (-343 mV *vs.* Ag/AgCl) and another one
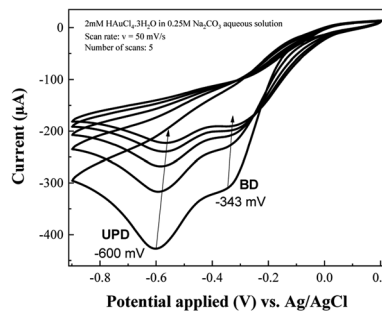

Fig. 1 Cyclic voltammograms recorded during the growth of gold nanoparticles on rGO/FTO.

attributed to underpotential deposition (UPD) (-600 mV *vs.* Ag/AgCl) of gold ions. The latter process is more related to the formation of adatom–substrate bond whereas the former one is attributed to the formation of adatom–adatom bond. Generally, it is hard to observe the UPD peak for bare electrode. And we might observe the UPD peak if the electrode is modified with a suitable material that is favoured to rapid metal nucleation. Similar results have been obtained for AuNPs grown on FTO electrode modified with PDA.[31] The intensities of both BD and UPD peaks were gradually decreased after every cycle due to the continuous decrease in local concentration of metallic ions nearby the electrode surface.[28]

SEM images for the bare FTO, rGO/FTO, AuNPs/rGO/FTO, and PDA/AuNPs/rGO/FTO are represented in Fig. 2. The bare FTO electrode shows a very rough surface. A thin and wrinkled film was observed on the electrode surface after being coated with electrochemically reduced graphene oxide. Indeed, it was generally reported that the rGO material often exhibits this flexible texture.[27,29,32] As seen in Fig. 2, the AuNPs has grown onto rGO/FTO electrode with average particle diameter estimated to be around 75 nm. Actually, AuNPs commonly tend to aggregate during the growth to generate particle clusters.[33] However, we have observed here the discrete particles instead of accumulated ones since the use of rGO supporting layer might have helped to prevent particle aggregation. Similar effects were
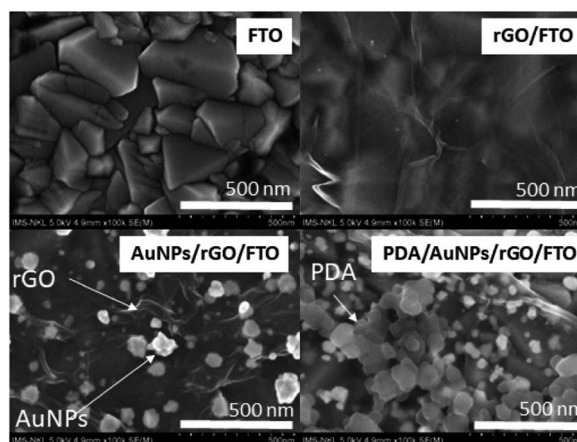

Fig. 2 SEM images of modified electrodes.

also observed once conducting polymers or thin organic layers were employed as supporting layers to electro-deposit metal nanoparticles.[28,34–36] Indeed, the large surface area of rGO with highly flexible texture might provide a sufficient number of nucleation sites for metallic nanoparticles.[26] In the same time, the residual functional groups (mainly hydroxyl, carboxylic) with negative charge can attract more metal ions from solution to the electrode surface *via* electrostatic interaction, thus increase the number of nucleation sites and also possibly enhance stability of the as-grown particles.[25] Finally, the highly porous PDA material was observed once PDA is present on the electrode surface. Similar morphology was also found on PDA film deposited directly on FTO electrode (not shown here) and PDA aggregates in solution (Fig S3†). The surface morphology of PDA based film is actually controlled by competition between aggregation in solution and deposition on the surface. At high dopamine concentration (>1 mg mL^{-1}), there are many aggregated particles generated on a thin PDA film with the thickness less than 20 nm.[37] It was also reported that the abundant hydroxyl groups in PDA are good capping and reductive agents for synthesis of gold nanoparticles on FTO electrode.[31] That explains the formation of a thin capping layer surrounding as-grown gold nanoparticles. To conclude, all these findings have firmly confirmed the generation of PDA/AuNPs/rGO film as expected. The chemical components of as-prepared films on FTO electrodes was first examined by EDX technique. The atomic weight of Au in the PDA/AuNPs/rGO/FTO hybrid film was estimated to be 4.31% (Table S1†).

XPS analysis was further conducted to reveal binding states of elements in the samples (Fig. 3). The survey XPS spectrum of PDA/AuNPs/rGO/FTO electrode shows presence of C, O, N, and Au elements. C 1s deconvoluted spectrum exhibits C–C (285.0

eV), C–O (286.3 eV) and C=O (288.7 eV). O 1s spectrum shows two common binding states of oxygen at 530.0 eV (O=C) and 531.5 (C–C) eV in organic compounds rich in oxygen-containing functional groups. High-resolution N 1s spectrum shows binding states of nitrogen with carbon atoms in indolic moieties in PDA. Au 4f deconvoluted spectrum indicated two featured peaks of Au 4f$_{5/2}$ (87.8 eV) and Au 4f$_{5/2}$ (84.2 eV).

Raman spectra of the samples were utilized to examine structural behaviors of the samples (Fig. 4). Two typical peaks located at 1595 cm^{-1} (G) and 1342 cm^{-1} (D) relevant to graphitic structure and defective structure of carbonaceous material[38] were observed in rGO/FTO. In the Raman spectrum of AuNPs/rGO modified electrode, we do obtain the two similar peaks, but the D peak is slightly shifted to lower wavenumber by 32 cm^{-1}. As mentioned above, the defective sites on graphite structure with possibly negative charges are more favorable for the nucleation and growth of gold nanoparticles. Probably, the observed peak shift is a clear evidence to confirm once more time the coordination between gold material and defects on graphite flakes. The sample PDA/AuNPs/rGO/FTO shows all characteristic features of both rGO and PDA materials, once more confirmed the successful preparation of the expected hybrid film. Actually, the PDA material containing indolic moieties also exhibits vibration peaks attributed to sp^2 carbon atoms (1561 cm^{-1}) and sp^3 carbon atoms (1320 cm^{-1}), and one more peak related to C–N bond (1409 cm^{-1}) (Fig S3†). The I_D/I_G ratio which indicates the defect level of graphite structures was also found to be increased from 1.70 (rGO/FTO) to 2.88 (AuNPs/rGO/FTO) and 2.78 (PDA/AuNPs/FTO). Consequently, the size graphite domain (estimated from empirical Tuinstra–Koenig relation[39]) is decreased from 11.3 nm (rGO/FTO) to 6.7 nm (AuNPs/rGO/FTO) and 6.9 nm (PDA/AuNPs/FTO). The high I_D/I_G ratio and small size of graphite domain in our samples might be resulted from limited reduction yield of graphene oxide on FTO electrodes and large number of layers in as-prepared rGO films.

Charge transfer resistance

Since we aim to develop an impedimetric sensor based on as-prepared hybrid film for cytosensing purpose, it is essential to
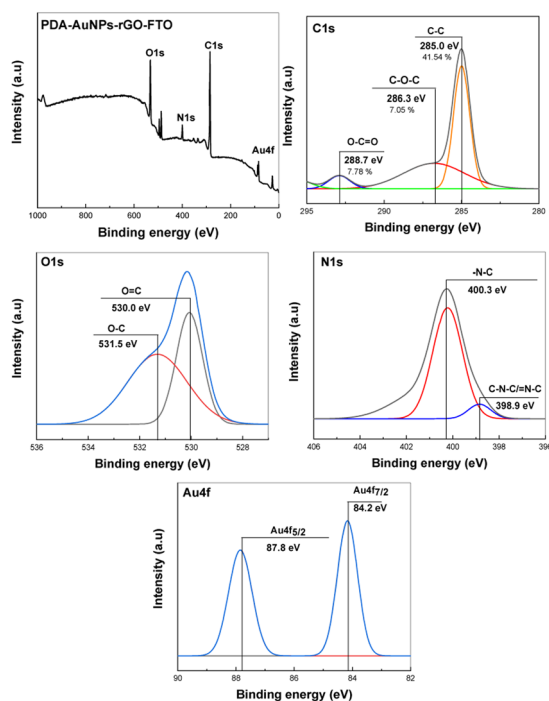

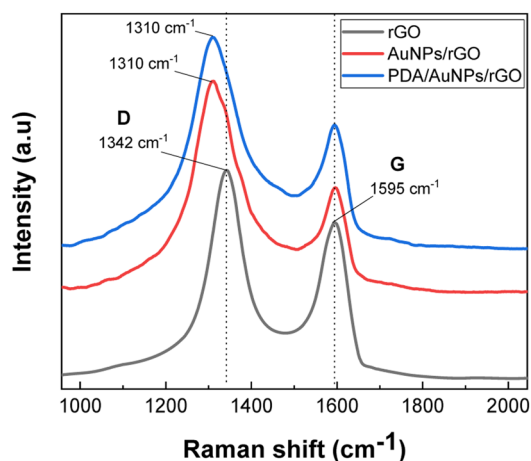Fig. 3 XPS analysis of modified electrodes.
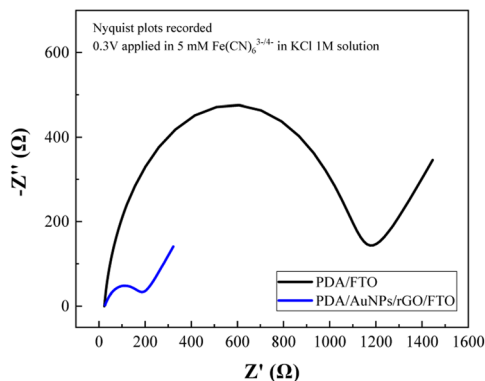

Fig. 4 Raman spectra of modified electrodes.

Fig. 5 EIS spectra recorded on PDA/FTO and PDA/AuNPs/rGO/FTO.

evaluate the charge transfer behavior of the hybrid film itself. The charge transfer resistance of PDA/FTO and PDA/AuNPs/rGO/FTO were determined from EIS spectra (Fig. 5) recorded in 1 M KCl solution containing 5 mM $Fe(CN)_6^{3-/4-}$.

As seen from Fig. 5, the recorded Nyquist plot contains a semi-circle and a linear line. While the semi-circular part at higher frequencies corresponds to the electron-transfer limited process, the linear part at lower frequencies represents the diffusion-controlled process.[40] In the impedance spectra, the diameter of semicircle indicates the electrode/solution interface resistance (or charge transfer resistance, denoted as R_{CT}), calculated by using Randles circuit model where R_S is the resistance of the electrolyte solution, C_{dl} is the double layer interfacial capacitance between the electrode and the solution, and Z_W as the Warburg impedance.

The charge transfer resistance of PDA film (1087 ± 2.2 Ω for PDA/FTO electrode) was found to be improved by six times with the AuNPs/rGO ad-layer (162.5 ± 2.7 Ω for PDA/AuNPs/rGO/FTO electrode). The presence of homogeneous gold nanoparticles decorated onto reduced graphene oxide flakes with relatively low charge transfer resistance (the semi-circle nearly disappear) is the reason behind this improvement in electron transfer behavior of the hybrid film. Moreover, the hybridization between gold material and carbonaceous supports at defect sizes (as observed in Raman spectra) might also contribute partly to the increase in electron transfer rate at electrode surface.[33] In deed, the electron transfer resistance of bare FTO and rGO/FTO electrodes are also very small (less than 50 Ω). The decrease in charge transfer resistance enables us to downscale the detection limit of the developing impedimetric cytosensor.

Cell viability – MTT test

The biocompatibility of PDA material was tested using MTT test against A-549 lung cancer cells. The PDA film was generated inside the 96-wells plate using the same method to produce PDA film onto electrode surface. The test was conducted at high cell concentration of 10^5 cells per mL. The optical density at 570 nm (related to formazan crystal) was measured for both non-modified plate (blank) and PDA modified plate (sample), and then the viability was determined as:
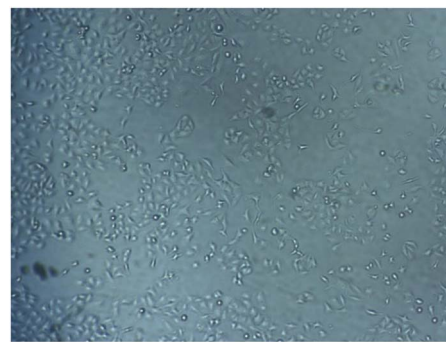

Fig. 6 Microscopy image of A-549 cells immobilized on polydopamine film (MTT test).

$$\% \ \text{Viability} = \frac{\text{mean OD}_{\text{sample}}}{\text{mean OD}_{\text{blank}}} \times 100$$

The viability of the cell was determined to be 98%. This result indicated that the PDA material exhibits no toxicity towards A-549 cells. It has been previously reported that PDA solution has no significant toxicity against HeLa cells[41] and PDA film displayed a viability of 112% towards A-549 cells.[23,42] The presence of A-549 cells with non-sphere morphology on the surface of the plate was also obtained on microscopy image (Fig. 6).

Cell detection

EIS technique was used to detect the tumor cells immobilized onto the electrode surface. We will first build the calibration curve on PDA/AuNPs/rGO/FTO electrode in concentration range from 10^1–10^4 cells per mL. The EIS spectra of PDA/AuNPs/rGO/FTO electrode incubated with A-549 cells at different concentrations are shown in Fig. 7. The recorded R_{CT} values were found to be increased with the increasing concentration of A-549 cells.

The relationship between the variation in charge transfer resistance and cell concentration is as follows: ΔR_{CT} (kΩ) = $0.1340 + 0.3570 \times \log(C$ (cells per mL)) ($R^2 = 0.9916$) (Fig. 8). The
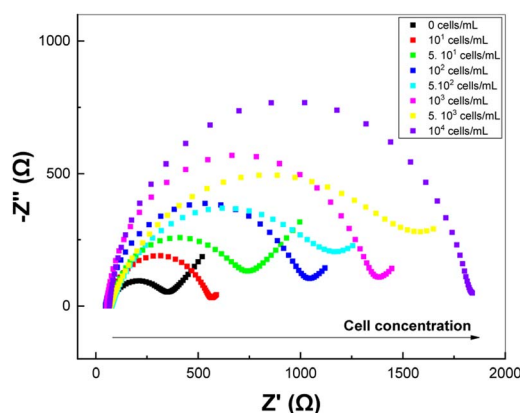

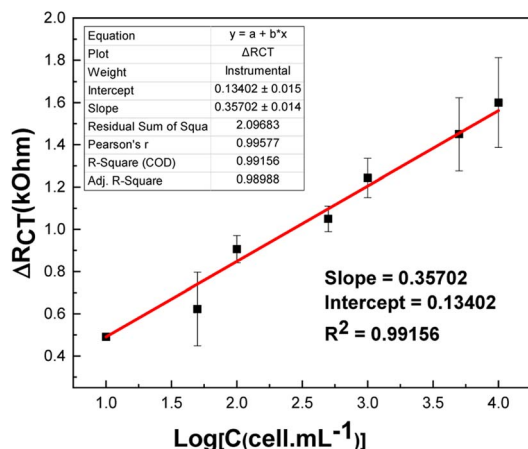**Fig. 7** EIS spectra recorded on PDA/AuNPs/rGO/FTO at different cell concentrations.

Fig. 8 Calibration curve.

detection limit ($3.3 \times S_y/S$, where S_y is the standard deviation and S is the slope of the calibration curve) was estimated to be 2 cells per mL. This value is comparable with those obtained in previous works (Table S2†).[23,26,43–45] Indeed, PDA has been reported to be a suitable material to develop electrochemical cytosensor for detection of A-549 due to the strong adhesion between PDA and receptor-rich tumor cells.[23] Also, the detection limit was improved by fourteen times compared with sensing platform without AuNPs/rGO ad-layer (Fig S5†). Compared with PDA/FTO sensor (Fig S5†), the electrochemical signals recorded on EIS spectra during cell detection are much more stable with much smaller errors and better R-square ($R^2 = 0.9977$).

Conclusions

In conclusion, PDA/AuNPs/rGO film has been successfully prepared onto FTO electrode for further application in A-549 detection. Gold discrete nanoparticles (75 nm) were electrodeposited onto electrode surface with the aid of rGO supporting layer. Later, this ad-layer becomes the matrix to grow PDA material from alkaline solution with less aggregates. The results have shown that the PDA material exhibits good adhesion and biocompatibility towards A-549 cells. Meanwhile, the introduction of AuNPs/rGO ad-layer has improved the electron transfer at electrode surface about six times. These findings allow us to further detect A-549 cells on as-developed electrochemical cytosensor based on PDA/AuNPs/rGO/FTO. The detection limit of the as-prepared sensor was 1 cells per mL. The final electrochemical cytosensor based on PDA/AuNPs/rGO films can be coupled with a cell size-based microfilter in near future to ensure the cell selectivity (the size of CTC cells is much larger than that of heathy cells).

Author contributions

All authors have given approval to the final version of the manuscript. The corresponding author Dr VU Thi Thu is in charge to implement all research activities and write the main manuscript. The first author Ms NGUYEN Dieu Linh is

responsible for all experiments related to prepare materials, elaborate sensing interfaces, and test sensing performances. Dr NGUYEN Hai Dang and Dr NGUYEN Trang Huyen support us on cell culture and MTT test. Prof. Benoit Piro provided us valuable advices for our experience design and also support us on XPS characterization of the samples.

Conflicts of interest

There are no conflicts to declare.

Acknowledgements

References

1 C. Jin, S. M. FcFaul, S. P. Duffy, X. Deng, P. Tavassoli, P. C. Black and H. Ma, Technologies for label-free separation of circulating tumor cells: from historical foundations to recent developements, *Lab Chip*, 2014, **14**(1), 32–44.

2 P. Chen, Y.-Y. Huang, K. Hoshino and X. Zhang, Multiscale immunomagnetic enrichment of circulating tumor cells: from tubes to microchips, *Lab Chip*, 2014, **14**, 446–458.

3 C.-H. Leung, K.-J. Wu, G. Li, C. Wu, C.-N. Ko and D.-L. Ma, Application of label-free techniques in microfluidic for biomolecules detection and circulating tumor cells analysis, *Trends Anal. Chem.*, 2019, **117**, 78–83.

4 N. Sun, X. Li, Z. Wang, Y. Li and R. Pei, High-purity capture of CTCs based on micro-beads enhanced isolation by size of epithelial tumor cells (ISET) method, *Biosens. Bioelectron.*, 2018, **102**, 157–163.

5 S. Hu, Z. Wang, Y. Gu, Y. Li and Y. Jia, Clinical available circulating tumor cell asssay based on tetra(4-aminophenyl) prophyrin mediated reduced graphene oxide field effect transistor, *Electrochim. Acta*, 2019, **313**, 415–422.

6 H.-X. Cao, P.-F. Liu, L. Wang, Z.-J. Liu, S.-Y. Ye and G.-X. Liang, Nonenzymatic chemiluminescence detection of circulating tumor cells in blood based on Au@luminol nanoparticles, hybridization chain reaction and magnetic isolation, *Sens. Actuators, B*, 2020, **318**, 128287.

7 P. Liu, L. Wang, K. Zhao, Z. Liu, H. Cao, S. Ye and G. Liang, High liminous efficiency Au@CDs for sensitive and label-free electrochemiluminescent dettection of circulating tumor cells in serum, *Sens. Actuators, B*, 2020, **316**, 128131.

8 J. Luo, L. Dong, D. Zhao and M. Yang, Photoelectrochemical detection of circulating tumor cells based on aptamer conjugated Cu2O as signal probe, *Biosens. Bioelectron.*, 2020, **151**, 111976.

9 C. Shen, L. Zhong, L. Xiong, C. Liu, L. Yu, X. Chu, X. Luo, M. Zhao and B. Liu, A novel sandwich-like cytosensor based on aptamer modified magnetic beads and carbon dots/cobalt oxyhydroxide nanosheets for circulating tumor cells detection, *Sens. Actuators, B*, 2021, **331**, 129399.

10 R. Tang, R. Hu, X. Jiang and F. Lu, LHRH-targeting surface-enhanced Raman scattering tags for the rapid detection of circulating tumor cells, *Sens. Actuators, B*, 2019, **284**, 468–474.

11 X. Huang, X. Hu, S. Song, D. Mao, J. Lee, K. Koh, Z. Zhu and H. X. Chen, Triple-enhanced surface plasmon resonance spectroscopy based on cell membrane and folic acid functionalized gold nanoparticles for dual-selective circulating tumor cell sensing, *Sens. Actuators, B*, 2020, **305**, 127543.

12 F. Li, G. Yang, Z. P. Aguilar, Y. Xiong and H. Xu, Affordable and simple method for separating and detecting ovarian cancer circulating tumor cells using BSA coated magnetic nanoprobes modified with folic acid, *Sens. Actuators, B*, 2018, **262**, 611–618.

13 X.-R. Li and Y.-G. Zhou, Electrochemical detection of circulating tumor cells: A mini review, *Electrochem. Commun.*, 2021, **124**, 106949.

14 H. Su, S. Yin, J. Yang, Y. Wu, C. Shi, H. Sun and G. Wang, In situ monitoring of circulating timor cell adhered on three-dimensional graphene/ZnO macroporous structure by resistance change and electrochemical impedance spectroscopy, *Electrochim. Acta*, 2021, **393**, 139093.

15 H. Zhang, H. Ke, Y. Wangg, P. Li, C. Huang and N. Jia, 3D carbon nanosphere and gold nanoparticles based voltammetric cytosensor for cell line A549 and for early diagnosis of non-small cell lung cancer cells, *Microchim. Acta*, 2019, **186**, 39.

16 S. Tang, H. Shen, Y. Hao, Z. Huang, Y. Tao, Y. Peng, Y. Guo, G. Xie and W. Feng, A novel cytosensor based on Pt@Ag nanoflowers and AuNPs/Acetylene back for ultrasensitive and highly specific detection of circulating tumor cells, *Biosens. Bioelectron.*, 2018, **104**, 72–78.

17 X.-Y. Wang, Y.-G. Feng, Ai-J. Wang, Li-P. Mei, P.-X. Yuan, X. Luo and J.-J. Feng, A facile ratiometric electrochemical strategy for ultrasensitive monitoring HER2 using polydopamine-grafted-ferrocene reduced graphene oxide, Au!Ag nanushuttles and hollow Ni@PtNi yolk-shcell nanocages, *Sens. Actuators, B*, 2021, **331**, 129460.

18 Y. Liu, H. Ma, J. Gao, D. Wu, X. Ren, T. Yan, X. Pang and Q. Wei, Ultrasensitive electrochemical immunosensor for SCCA detection based on ternary Pt/PdCu nanocube anchored on three-dimensional graphene framework for signal amplification, *Biosens. Bioelectron.*, 2016, **79**, 71–78.

19 F. Li, J. Han, L. Jiang, Y. Wang, Y. Li, Y. Dong and Q. Wei, An ultrasensitive sandwich-type electrochemical immunosensor based on signal amplification strategy of gold nanoparticles functionalized magnetic multi-walled carbon nanotubes loaded with lead ions, *Biosens. Bioelectron.*, 2015, **68**, 626–632.

20 J. Yang, X. Huang, C. Gan, R. Yuan and Y. Xiang, Highly specific and sensitive point-of-care detection of rare circulating tumor cells in whole blood via a dual recognition strategy, *Biosens. Bioelectron.*, 2019, **143**, 111604.

21 M. Sadeghi, S. Kashanian, S. M. Naghib and E. Arkan, A high-performance electrochemical aptasensor based on graphene-decorated rhodium nanoparticles to detect HER2-ECD oncomarker in liquid biopsy, *Sci. Rep.*, 2022, **12**, 3299.

22 X. Zhou, Y. Li, H. Wu, W. Huan, H. Ju and S. Ding, An amperometric immunosensor for sensitive detection of circulating tumor cells using a tyramide signal amplification - based signal enhancement system, *Biosens. Bioelectron.*, 2019, **130**, 88–94.

23 G. Bolat, O. A. Vural, Y. T. Yaman and S. Abaci, Polydopamine nanoparticles-assisted impedimetric sensor towards label-free lung cancer cell detection, *Mater. Sci. Eng., C*, 2021, **119**, 111549.

24 H. Lee, S. M. Dellatore, W. M. Miller and P. B. Messersmith, Mussel-inspired surface chemistry for multifunctional coatings, *Science*, 2007, **318**, 426–430.

25 G. H. Jin, E. Ko, M. K. Kim, V.-K. Tran, S. E. Son, Y. Geng, W. Hur and G. H. Seong, Graphene oxide - gold nanozyme for highly sensitive electrochemical detection of hyrogen peroxide, *Sens. Actuators, B*, 2018, **274**, 201–209.

26 A. Zhang, Q. Liu, Z. Huang, Q. Zhang, R. Wang and D. Cui, Electrochemical cytosensor based on a gold nanostar-decorated graphene oxide platform for gastric cancer cell detection, *Sensors*, 2022, **22**(7), 2783.

27 V. C. Nhung, N. N. Tien, D. T. N. Nga, P. D. Chung, N. T. T. Ngan, V. C. Tu and V. T. Thu, Facile preparation of highly uniform and stable AuNPs/rGO-PEDOT:PSS hyrbid film for electrochemical detection pf pharmaceutical residue in water, *Journal of Nanoparticle Research*, 2022, **24**, 34.

28 T. T. Vu, T. N. N. Dau, C. T. Ly, D. C. Pham, T. T. N. Nguyen and V. T. Pham, Aqueous electrodeposition of (AuNPs/MWCNT-PEDOT) composite for high-affinity acetylcholinesterase electrochemical sensors, *J. Mater. Sci.*, 2020, **55**, 9070–9081.

29 V. T. Thu, B. Q. Tien, D. T. N. Nga, L. C. Thanh, L. H. Sinh, T. C. Le and T. D. Lam, Reduced graphene oxide - polyaniline film as enhanced sensing interface for the detection of loop-mediated-isothermal-amplification products by open circuit potential measurement, *RSC Adv.*, 2018, **8**, 25361.

30 T. T. Vu, M. Fouet, A.-M. Gue and J. Sudor, A new and easy surface functionalization technology for monitoring wettability in heterogeneous nano- and microfluidic devices, *Sens. Actuators, B*, 2014, **196**, 64–70.

31 W. Ye, D. Wang, H. Zhang, F. Zhou and W. Liu, Electrochemical growth of flowerlike gold nanoparticles on polydopmine modified FTO glass for SERS application, *Electrochim. Acta*, 2010, **55**, 2004–2009.

32 L. C. Thanh, D. T. N. Nga, N. V. B. Lam, P. D. Chung, L. T. T. Nhi, L. H. Sinh, V. T. Thu and T. D. Lam, Acetylcholinesterase sensor based on PANi/rGO film electrochemically grown on screen-printed electrodes, *Vietnam J. Chem.*, 2021, **59**(2), 253–262.

33 H. Yin, H. Tang, D. Wang, Y. Gao and Z. Tang, Facile synthesis of surfactant free Au cluster graphene hybrids for high-performance oxygen reduction reaction, *ACS Nano*, 2012, **6**(9), 8288–8297.

34 L. Devkota, L. T. Nguyen, T. T. Vu and B. Piro, Electrochemical determination of tetracycline using AuNP-coated molecularly imprinted overoxidized polypyrrole sensing interface, *Electrochim. Acta*, 2018, **270**, 535–542.

35 N. T. Hoang, P. T. T. Nguyen, P. D. Chung, V. T. T. Ha, T. Q. Hung, P. T. Nam and V. T. Thu, Electrochemical preparation of monodisperse Pt nanoparticles on a grafted 4-aminothiophenol supporting layer for improving the MOR reaction, *RSC Adv.*, 2022, **12**, 8137.

36 R. Ayranci, B. Demirkan, B. Sen, A. Savk, M. Ak and F. Sen, Use of the monodisperse Pt/Ni@rGO nanocomposite synthesized by ultrasonic hydroxide assisted reduction method in electrochemical nonenzymatic glucose detection, *Mater. Sci. Eng., C*, 2019, **99**, 951–956.

37 Y. Ding, Lu-T. Weng, M. Yang, Z. Yang, X. Lu, N. Huang and L. Yang, Insights into the aggregation/deposition and structure of a polydopamine film, *Langmuir*, 2014, **30**, 12258–12269.

38 C. Gomez-Navarro, R. T. Weitz, A. M. Bittner, M. Scolari, A. Mews, M. Burghard and K. Kern, Electronic transport properties of individual chemically reduced graphene oxide sheets, *Nano Lett.*, 2007, **7**(11), 3499–3503.

39 F. Tuinstra and J. L. Koenig, Raman spectrum of graphite, *J. Chem. Phys.*, 1970, **53**, 1126.

40 E. P. Randviir and C. E. Banks, Electrochemical impedance spectroscopy: an overview of bioanalytical applications, *Anal. Methods*, 2013, **5**, 1098–1115.

41 J. Tan, Z. Xie, Z. Zhang, Y. Sun, W. Shi and D. Ge, Dopamine modified polyaniline with improved adhesion, dispersibility, and biocompatibility, *J. Mater. Sci.*, 2018, **53**, 447–455.

42 F. Aysin, A. Yilmaz and M. Yilmaz, Metallic nanoparticle decorated polydopamine thin films and their cell proliferation charactertistics, *Coatings*, 2020, **10**(9), 802.

43 J. Cai, H. Shen, Y. Wang, P. Yang, S. Tang, Y. Zhu, Q. Liu, B. Li, G. Xie and W. Feng, A dual recognition strategy for accurate detection of CTCs based on novel branched PtAuRh trimetallic nanospheres, *Biosens. Bioelectron.*, 2021, **176**, 112893.

44 H. Xu, J. Zheng, H. Liang and C.-P. Li, Electrochemical sensor for cancer cell detection using calix[8]arene/polydopamine/phosphorene nanocomposite on host-guest recognition, *Sens. Actuators, B*, 2020, **317**, 128193.

45 Y. Chen, J. Peng, Y. Lai, B. Wu, L. Sun and J. Weng, Ultrasensitive label-free detection of circulating tumor cells using conductivity matching of two-dimensional semicondcutor with cancer cell, *Biosens. Bioelectron.*, 2019, **124**, 111520.